Physically Realizable Space for the Purity-Depolarization Plane for Polarized Light Scattering Media

Aziz Tariq,[1,2] Pengcheng Li,[1,2] Dongsheng Chen,[1,2] Donghong Lv,[1,4] and Hui Ma[1,2,3,*]
[1]Shenzhen Key Laboratory for Minimal Invasive Medical Technologies, Institute of Optical Imaging and Sensing, Graduate School at Shenzhen, Tsinghua University, Shenzhen 518055, China
[2]Department of Physics, Tsinghua University, Beijing 100084, China
[3]Center for Precision Medicine and Healthcare, Tsinghua-Berkeley Shenzhen Institute, Shenzhen 518071, China
[4]Department of Biomedical Engineering, Tsinghua University, Beijing 100084, China
(Received 16 February 2017; published 21 July 2017)

We propose a physically realizable space for the polarized light scattering measurement using the Stokes-Mueller formalism by a purity-index–depolarization-index ($\mathrm{PI} - P_\Delta$) plane. The parameter PI is defined from indices of polarimetric purity (IPP), which exhibits the overall magnitude of the polarimetric randomness of a medium, while the depolarization index (P_Δ) delineates a proper global degree of polarimetric purity and may also refer to the average measure of depolarization power of the scattering medium. Subregions and curves connecting the edge points in the plane are obtained by imposing certain constraints on the IPP; consequently any point on the subregion indicates the information related to a decomposition of the Mueller matrix into its components as a convex sum. From the same set of constraints, complete information about the depolarization index versus the entropy $[S(\mathbf{M}) - P_\Delta]$ diagram is recovered. This work provides a simple geometric representation and a deeper perceptivity of the light scattering media comprising depolarization.

DOI: 10.1103/PhysRevLett.119.033202

Introduction.—Polarized light scattering measurements have played a central role in understanding the microscopic specific features of a medium and caused a lot of interest in several fields of science and technology such as astronomy, metrology, and biomedical optics [1–3]. When polarized light interacts with a medium, it may suffer multiple scattering and subsequently gets partially or fully depolarized. The depolarization behavior of light can be well studied through the Stokes-Mueller formalism, and the so-called depolarization index (or the degree of polarimetric purity) (P_Δ) can be obtained from elements of a Mueller matrix $\mathbf{M}$ of the medium [4]. P_Δ can have a maximum value of 1, which shows that there is no change in the degree of polarization of incident light after the interaction, while the minimum value of 0 corresponds to a complete depolarization. From $\mathbf{M}$, a Hermitian covariance matrix ($\mathbf{H}$) can be constructed whose eigenvalues are used to calculate the polarization entropy ($S(\mathbf{M})$), which provides information about the average entropy added to the field after the interaction with the medium. The polarization entropy has a range of $0 \leq S(\mathbf{M}) \leq 1$. The maximum can be associated to a complete depolarization, whereas the minimum value can be related to a pure Mueller matrix [2,5–7].

A physical bound to the $S(\mathbf{M}) - P_\Delta$ relation based on random uniform distributions of the normalized eigenvalues of $\mathbf{H}$ was given by Aiello and Woerdman [7]. Analytical expressions for curves joining the cusps in the plane were derived. Experimental confirmation for Ref. [7] was presented [8] by measuring the $\mathbf{M}$ of a large class of scattering media in forward detections. The experimental data filled in all the regions except a subregion that remained empty [8]. An alternate approach to characterize the universality in depolarized light scattering was published [9] by a simulation based on the statistical properties of $\mathbf{M}$ to recover the experimental distribution in $S(\mathbf{M}) - P_\Delta$ plane. An attempt was made to explain the empty region by imposing a physical criterion that the region may be represented by a region of "anomalous depolarization" defined as both the cross-polarization ratios greater than 1. However, this criterion was not a universal constraint, also pointed out by the authors [9]. On the other hand, three invariant "indices of purity" (IPP) were defined [2,10,11] from the eigenvalues of $\mathbf{H}$ to describe the information relevant to the polarimetric randomness (or, conversely, purity) of the medium for the four-dimensional (4D) polarized light, and a three-dimensional plot for a feasible region called the 4D purity space was formed. Recently, another illustration, namely, the "purity figure" based on the degree of polarizance and the degree of spherical purity was studied [12] for the description of the polarized light scattering from media.

In this Letter, a scalar parameter named the overall purity index (PI) is defined from the IPP and the 4D purity space, which can be related to the overall magnitude of purity of the medium. Since PI is a multivalued function of P_Δ, thus a physically realizable two-dimensional $\mathrm{PI} - P_\Delta$ plot for all the light scattering media is generated. The "trivial" or "characteristic decomposition" (CD) of the $\mathbf{M}$ in which the coefficients of the mutually incoherent components are given in terms of the IPP [11] is employed to designate the subregions and the curves of the plane as a linear combination of the components of $\mathbf{M}$. Furthermore, Monte Carlo simulations based on a sphere model in both the forward and backscattering detections [13–16] for spheres with varying

sizes and scattering coefficients in the Mie regime are employed to correlate the simulation results to the descriptions of the subregions in terms of the IPP and CD.

The purity-depolarization plane.—For a quasimonochromatic optical field of zero-mean variable that can be considered as an ergodic stochastic stationary process (at least in the wide sense) whose direction of propagation is constant in time at a point $\mathbf{r}$ and with a Gaussian spectral profile such that the second order statistical moments are sufficient, a two-dimensional (2D) positive semidefinite (PSD) coherency matrix ($\mathbf{\Phi}_2$) is ciphered for the complete description of the two-dimensional (2D) polarized light [2,6,17,18]. In the 2D description of the polarized light, it is considered that the polarization ellipse may change uniformly or randomly but remains fixed in a plane with constant direction of propagation. If the direction of propagation is not fixed, a three-dimensional (3D) polarized light is considered, whose associated PSD covariance matrix is the three-dimensional (3D) coherency matrix ($\mathbf{\Phi}_3$) [2,18]. Usually, a dimensionless density matrix is used via considering $\mathbf{D}_N = \frac{\mathbf{\Phi}_N}{\mathrm{tr}(\mathbf{\Phi}_N)}$, where N is the dimension of the matrix, with "tr" standing for the trace [18]. The density matrix can be represented in terms of the Stokes parameters. In general, a 4×4 Mueller matrix $\mathbf{M}$ of the medium is used to describe the transformation of a Stokes vector of the polarized light interacting with the scattering medium. A four-dimensional (4D) coherency matrix $\mathbf{C}$ and the covariance matrix $\mathbf{H}$ can be constructed from elements of the $\mathbf{M}$ via exploiting their Hermiticity and symmetry properties [2,19]. Both matrices are PSD, and are related through unitary transformation. The covariance matrix is written as $\mathbf{H} = \frac{1}{4}\sum_{\mu\nu=1}^{4} m_{\mu\nu}\mathbf{E}_{\mu\nu}$, where $m_{\mu\nu}$ are the elements of the $\mathbf{M}$, and $\mathbf{E}_{\mu\nu}$ are the 16 modified Dirac matrices [2]. Moreover, any physically realizable $\mathbf{M}$ that contains depolarization can be decomposed up to four passive Mueller-Jones matrices ($\mathbf{M}_{J_i}$) as $\mathbf{M} = \sum_{i=1}^{4} \lambda_i \mathbf{M}_{J_i}$ [20,21]. For a Mueller matrix $\mathbf{M}$, $\forall\ \chi_i$ and ψ_i (ellipticity and orientation angles of polarization ellipse) such that the gain constraint $[0 \le g(\chi_i, \psi_i) \le 1]$ and the polarization constraint $[0 \le P_o(\chi_i, \psi_i) \le 1]$ are satisfied [6]. A Mueller matrix is considered as a physically realizable $\mathbf{M}$, if the eigenvalues of the $\mathbf{H}(\mathbf{M})$ are positive (Cloude criterion) [22] and the gain constraint is satisfied in both the forward and reverse directions [23]. Additionally, the three invariant "indices of polarimetric purity" (IPP) are defined as $P_1 = [(\lambda_1 - \lambda_2)/\mathrm{tr}(\mathbf{H})]$, $P_2 = [(\lambda_1 + \lambda_2 - 2\lambda_3)/\mathrm{tr}(\mathbf{H})]$, and $P_3 = [(\lambda_1 + \lambda_2 + \lambda_3 - 3\lambda_4)/\mathrm{tr}(\mathbf{H})]$ ($\mathrm{tr}(\mathbf{H}) = m_{11} = 1$ for a normalized $\mathbf{M}$ with $\sum_{i=1}^{4} \lambda_i = 1$) [10,11]. From the eigenvalue spectrum of the $\mathbf{H}$ in the form $\lambda_1 \ge \lambda_2 \ge \lambda_3 \ge \lambda_4$ the following inequality is obtained:

$$0 \le P_1 \le P_2 \le P_3 \le 1. \tag{1}$$

Furthermore, $\mathbf{M}$ can be decomposed into a linear combination of a pure and depolarizing Mueller matrices in a form called characteristic decomposition (CD) [2,11]. The CD of a normalized $\mathbf{M}$ in terms of the IPP is written as

$$\mathbf{M} = P_1(\mathbf{M}_{J1}) + (P_2 - P_1)\mathbf{M}_2 + (P_3 - P_2)\mathbf{M}_3 + (1 - P_3)\mathbf{M}_4. \tag{2}$$

Here, $\mathbf{M}_{J1}$ is the Mueller-Jones matrix, which is constructed by considering $\mathbf{H}$ such that it contains only one eigenvalue in the spectral decomposition. Similarly, $\mathbf{M}_2$, $\mathbf{M}_3$, and $\mathbf{M}_4$ are the 2D, 3D, and complete (4D) depolarizers obtained by considering an equal probable mixture of the two, three, and all the four eigenvalues of $\mathbf{H}$ of $\mathbf{M}$, respectively. Moreover, P_1 can be inferred as the degree of polarization of $\mathbf{M}$ such that it is the relative portion of the system that can be considered $\mathbf{M}_{J1}$ in the CD. On similar footings, P_2 and P_3 are associated with the degree of 2D and 3D polarizations of the $\mathbf{M}$ in the CD [2]. It is worth mentioning that the Cloude criterion with the CD can be exploited for the noise filtering in the measurements [24]. Based on the description of the IPP, a quantity of the overall purity index with equal weights in the quadratic average to measure the overall purity of the medium is defined as

$$\mathrm{PI} = \sqrt{\frac{(P_1^2 + P_2^2 + P_3^2)}{3}}. \tag{3}$$

The range of PI is $0 \le \mathrm{PI} \le 1$. The minimum value of PI represents a Mueller matrix of a complete depolarizer ($\mathbf{M}_4$: 4D depolarizer) with only the first element m_{11} equal to 1 and the rest of all being zero, while the maximum value of the PI, i.e., 1 is for a pure $\mathbf{M}$ ($\mathbf{M}_J$, Mueller-Jones matrix). P_Δ can also be expressed in terms of the IPP as [2],

$$P_\Delta = \sqrt{\frac{1}{3}\left(2P_1^2 + \frac{2}{3}P_2^2 + \frac{1}{3}P_3^2\right)}. \tag{4}$$

Since the PI and P_Δ are functions of the IPP together with the inequality [Eq. (1)], and considering a random uniform distribution of the IPP, a two-dimensional physically realizable space for all the light scattering media is generated [Fig. 1(a)]. In lieu, PI = PI (P_Δ, P_α) as a multivalued function of P_Δ can be expressed to generate the same plot, where P_α is a combination of the remaining two IPP after eliminating any one of the IPP. Subregions in Figs. 1(a) and 1(b) (regions I, II, III, and IV) of the planes are separated by curves that are generated by imposing certain constraints (listed in Table I) on the IPP in Eqs. (3) and (4). The constraints on the IPP for producing the feasible subregions are given in Table II. Interestingly, $S(\mathbf{M})$ can be expressed as $S(\mathbf{M}) = -\frac{1}{4}[\{S_A(\log_4(S_A) - 1)\} + \{S_B(\log_4(S_B) - 1)\} + \{S_C(\log_4(S_C) - 1)\} + \{S_D(\log_4(S_D) - 1)\}]$, where $S_A = 1 + 2P_1 + \frac{2}{3}P_2 + \frac{1}{3}P_3$, $S_B = 1 - 2P_1 + \frac{2}{3}P_2 + \frac{1}{3}P_3$, $S_C = 1 - \frac{4}{3}P_2 + \frac{1}{3}P_3$, and $S_D = 1 - P_3$ [2,10]. Thus, from the same constraints on the IPP, the $S(\mathbf{M}) - P_\Delta$ plane is recovered as shown in Fig. 1(b) where the subregions and

TABLE I. Curves connecting the edge points in the $\mathrm{PI}-P_\Delta$ plane and the cusps in the $S(\mathbf{M})-P_\Delta$ plane.

	IPP				
Curves	P_1	P_2	P_3	CD	PI
C_{AB}	0	0	$0 \le P_3 \le 1$	$P_3\mathbf{M}_3 + (1-P_3)\mathbf{M}_4$	$0 \le \mathrm{PI} \le 1/\sqrt{3}$
C_{BC}	0	$0 \le P_2 \le 1$	1	$P_2\mathbf{M}_2 + (1-P_2)\mathbf{M}_3$	$1/\sqrt{3} \le \mathrm{PI} \le \sqrt{2/3}$
C_{CD}	$0 \le P_1 \le 1$	1	1	$P_1\mathbf{M}_{J1} + (1-P_1)\mathbf{M}_2$	$\sqrt{2/3} \le \mathrm{PI} \le 1$
C_{AC}	0	$0 \le P_2 = P_3 \le 1$		$P_2\mathbf{M}_2 + (1-P_2)\mathbf{M}_4$	$0 \le \mathrm{PI} \le \sqrt{2/3}$
C_{BD}	$0 \le P_1 = P_2 \le 1$		1	$P_1\mathbf{M}_{J1} + (1-P_1)\mathbf{M}_3$	$1/\sqrt{3} \le \mathrm{PI} \le 1$
C_{AD}	$0 \le P_1 = P_2 = P_2 \le 1$			$P_1\mathbf{M}_{J1} + (1-P_1)\mathbf{M}_4$	$0 \le \mathrm{PI} \le 1$

the curves are defined in terms of the IPP rather than the anlytical expression given in Ref. [7].

The subregion I (area BCD) in Figs. 1(a) and 1(b), where $P_3 = 1$, in which $\mathbf{M}$ of a medium can be decomposed up to a maximum of three pure Mueller matrices. From the CD [Eq. (2)], the region I may contain $\mathbf{M}_{J1}$, 2D, and 3D depolarizers. Here, the contribution of the 4D depolarizer ($\mathbf{M}_4$) is not included in the convex sum. This is evident from the planes as the region is not connected to the point A in the plane. The region II (the area ABC) is the region where $P_1 = 0$ stipulates that the first two dominant eigenvalues of the spectrum of $\mathbf{H}$ are equal. The region can be decomposed up to four pure matrices. By letting $P_1 = 0$ in Eq. (2), the region can be characterized as a linear combination of 2D, 3D, and 4D depolarizers with no contribution from $\mathbf{M}_{J1}$. In region III, $P_1 = P_2$, whereas in region IV, $P_2 = P_3$. Mueller matrices from the both regions can be decomposed up to four components, with equal contributions of the second and third components in region III, and the third and fourth components in region IV. Again, by putting the constraints of regions III and IV in Eq. (2), it is incurred that the former represents a linear combination of the $\mathbf{M}_{J1}$, 3D, and 4D depolarizers and the latter is composed of $\mathbf{M}_{J1}$, 2D, and 4D depolarizers. If the values of the IPP do not hold any of the constraint (i.e., $0 < P_1 < P_2 < P_3 < 1$) of the points inside the tetrahedron in the 4D space [10] then the inequalities will become approximations. However, CD can still be applied to provide the information about the relative portions of the components of the system. If $P_2 - P_1$ has a small magnitude then the contribution from $\mathbf{M}_2$ would be negligible, and if P_3 and P_2 has a small difference, the contribution from $\mathbf{M}_3$ would be insignificant in the CD. The contributions of $\mathbf{M}_{J1}$ and $\mathbf{M}_4$ become small for the cases when P_1 and P_3 are close to 0 and 1, respectively. It is worth noting that points A, B, C, and D can be represented by $\mathbf{M}_4$, $\mathbf{M}_3$, $\mathbf{M}_2$, and $\mathbf{M}_{J1}$, respectively, with an elegant geometrical representation if one is missing in the subregion.

The CD provides an insight for the physical meaning of the curves in the plane. For example, by letting $P_1 = 0$, $0 < P_2 < 1$, and $P_3 = 1$ in Eq. (2), it can be deduced that the curve C_{BC} represents a feasible region for the 3D depolarizer: a polarization ellipse that is not fixed in a plane and changes randomly. This could be bobbed up if an experimenter pays attention to study the polarization phenomena in fluctuating near fields and evanescent waves [10,18]. Note that the curve C_{BC} (for a mixed 3D polarization) is not connected to the points A and D, and, hence, cannot be decomposed into a pure and unpolarized light [18]. The curve C_{AD} is generated by taking all the values of the IPP equally, and, hence, characterizes a region that can be decomposed into a polarized and unpolarized light such that $P_1\mathbf{M}_{J1} + (1-P_1)\mathbf{M}_4$. It is an isotropic curve, which is a lower bound to the values of PI in the $\mathrm{PI}-P_\Delta$ plane with the unit slope and an upper bound to $S(\mathbf{M})$ in the $S(\mathbf{M})-P_\Delta$ plane. The advantage of the $\mathrm{PI}-P_\Delta$ plane over the $S(\mathbf{M})-P_\Delta$ plane is to avoid the logarithmic evaluation in the $S(\mathbf{M})$ measurement that can be sometimes cumbersome in calculating $S(\mathbf{M})$ for adjacent $n \times n$ windows of every pixel, which can be in the millions for the polarimetric synthetic aperture radar imaging [25] or in polarized light tissue imaging [26].

The analysis for light depolarization by scattering media via the $\mathrm{PI}-P_\Delta$ *plane.*—We discuss three cases of the elastic light scattering from media for the analysis and interpretation of the depolarization properties of the scattering media in terms of the IPP and the CD: (a) an experimentally measured Mueller matrix $\mathbf{M}_a$ of a dielectric underwater target [6,27]; and the two generic forms of Mueller matrices for (b) identical spherical scatterers $\mathbf{M}_b$

TABLE II. Subregions of the planes with the constraints on the IPP for $\mathrm{PI}-P_\Delta$ and $S(\mathbf{M})-P_\Delta$ planes.

	IPP				
Regions	P_1	P_2	P_3	CD	PI
I: Area BCD	$0 \le P_1 \le P_2 \le 1$		1	$P_1\mathbf{M}_{J1} + (P_2-P_1)\mathbf{M}_2 + (1-P_2)\mathbf{M}_3$	$1/\sqrt{3} \le \mathrm{PI} \le 1$
II: Area ABC	0	$0 \le P_2 \le P_3 \le 1$		$P_2\mathbf{M}_2 + (P_3-P_2)\mathbf{M}_3 + (1-P_3)\mathbf{M}_4$	$0 \le \mathrm{PI} \le \sqrt{2/3}$
III: Area ABD	$0 \le P_1 = P_2 \le P_3 \le 1$			$P_1\mathbf{M}_{J1} + (P_3-P_1)\mathbf{M}_3 + (1-P_3)\mathbf{M}_4$	$0 \le \mathrm{PI} \le 1$
IV: Area ACD	$0 \le P_1 \le P_2 = P_3 \le 1$			$P_1\mathbf{M}_{J1} + (P_2-P_1)\mathbf{M}_2 + (1-P_2)\mathbf{M}_4$	$0 \le \mathrm{PI} \le 1$

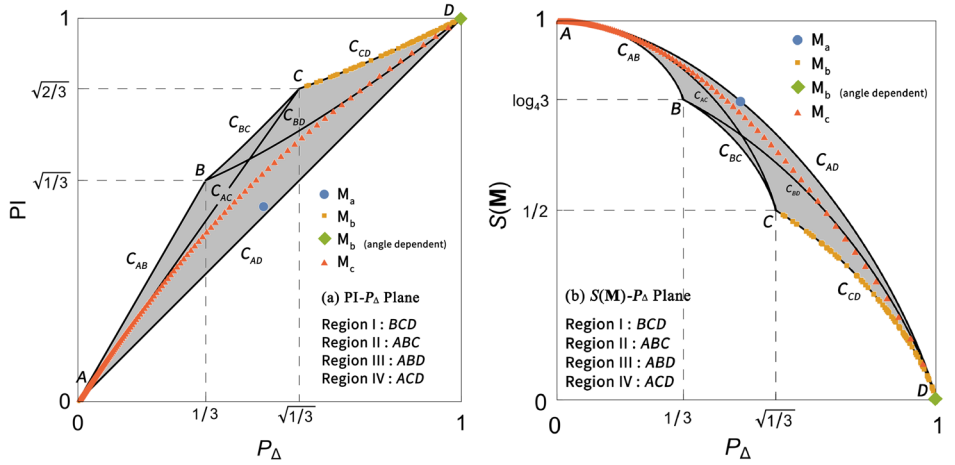

FIG. 1. Feasible spaces with curves for (a) the PI $-$ P_Δ plane with the edge points A (0, 0), B (1/3, $1/\sqrt{3}$), C ($1/\sqrt{3}$,$\sqrt{(2/3)}$), and D (1,1). (b) The $S(\mathbf{M}) - P_\Delta$ plane with the cusp points A (0, 1), B [1/3,$\log_4(3)$], C ($1/\sqrt{3}$,1/2), and D (1, 0). The regions I, II, III, and IV are specified by the areas BCD, ABC, ABD, and ACD, respectively. $\mathbf{M}_a$ is the experimentally measured matrix, Ref. [27], whereas $\mathbf{M}_b$ and $\mathbf{M}_c$ are generated from the formulations given in Refs. [6,27,28].

[6,27], which is a block diagonal Mueller matrix (with $m_{11} = m_{22}$, $m_{12} = m_{21}$, $m_{34} = -m_{43}$, and $m_{33} = m_{44}$); and (c) Rayleigh spheres with multiple scattering, which is a diagonal matrix $\mathbf{M}_c = \mathrm{diag}[1, m_{22}(n), m_{22}(n), m_{44}(n)]$, where $n+1$ is the number of scattering events. The detailed formulations of these Mueller matrices are given in Refs. [6,28]. A set of matrices $\mathbf{M}_b$ are constructed by generating random uniform numbers and satisfying Eq. (1), whereas the set of $\mathbf{M}_c$ are obtained by considering the values of n from zero to 16 (total of 160 points). The points on the planes as shown in Figs. 1(a) and 1(b) are obtained by calculating the values of the IPP from the Mueller matrices.

The IPP spectrum of the $\mathbf{M}_a$ [0.4672, 0.4905, and 0.5636] indicates that $P_1 \cong P_2$, thus lies in the region III close to the curve C_{AD}. Further employing the CD, it can be deduced that the relative portions of the 2D and 3D polarized light are very small; hence, depolarization in $\mathbf{M}_a$ arises mainly due to the combination of $\mathbf{M}_{J1}$ and the 4D depolarizer [6,27]. All the points for the $\mathbf{M}_b$ lie on the curve C_{CD}, except at the point C, and indicate that the $\mathbf{M}_b$ is a Mueller-Jones matrix [6]. If the elements of the $\mathbf{M}_b$ are angle dependent, only the one point at D is observed, which shows that these scatterers belong to the $\mathbf{M}_{J1}$ at all angles [6]. We then consider $\mathbf{M}_c$, which is formulated by Bicout and Brosseau [28] based on a maximum entropy principle. It is displayed that all the points lie in the region III for $n \geq 1$, and in the region I for $n \leq 1$, and move from the points D to A monotonically by increasing n. When n goes to large values (i.e., $n \geq 10$), we observe that the values for $\mathbf{M}_c$ reach closer to the 4D depolarizer ($\lim_{n\to\infty}\mathbf{M}_c = 4\mathrm{D}$) that is consistent with the findings of Ref. [28].

Monte Carlo simulations based on the sphere model.— We now conduct Monte Carlo (MC) simulations for the propagation of polarized photons in both forward and backward scattering with a model that contains monodispersed spherical scatterers in the Mie regime. The diameter d of the scatterers is increased for the scattering coefficients (μ_s) of 5, 10, and 15 cm^{-1}. Details of the MC program are given in Refs. [13–16]. Approximately, 10^7 photons at 0.63 μm wavelength are simulated with the medium of thickness 1 cm. The refractive indices for the medium and the sphere scatterers are 1.33 and 1.59, respectively. The preponderant forward scatterings (red points) in Fig. 2 occupy region IV and display a linear increase in the PI (or decrease in the entropy of the scatterers [29]) for large diameters. However, the backward scatterings (blue points) lie in the region II and show some parametric curves for the values of PI to the corresponding change in d, as shown in Fig. 2. It is observed that the "empty" region encountered in Ref. [8] is filled in for the backscattering spheres in the Mie regime. Thence, the region is more appropriately characterized as the region with 2D, 3D, and 4D depolarizations.

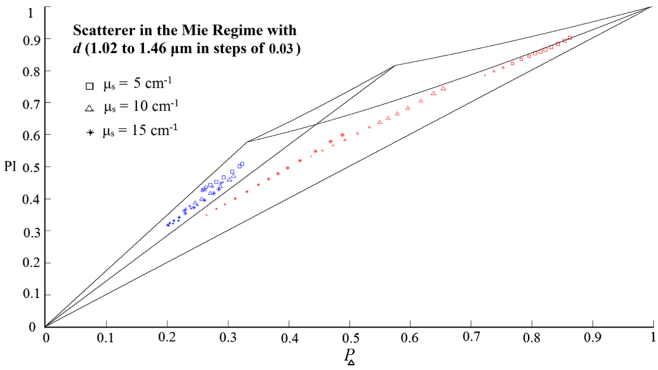

FIG. 2. MC simulations for spherical scatterers in forward- (red points) and backscattering (blue points) in the Mie regime with diameters increased from 1.02 to 1.46 μm in steps of 0.03. The scattering coefficients are 5 (square), 10 (triangle), and 15 (asterisk) cm^{-1}. The increase in the size of the scatterer is shown by increasing the size of the points.

We have used the $\mathrm{PI} - P_\Delta$ plane because of its simple geometric representation; however, one can use the $S(\mathbf{M}) - P_\Delta$ plane equally. Then the plane would be characterized by $S(\mathbf{M})$, P_Δ, and the IPP as the relative portions of the components of the system through CD.

Conclusion.—In summary, a 2D feasible ($\mathrm{PI} - P_\Delta$) plot is proposed for the description and characterization of depolarization properties of the scattering media. Both PI and P_Δ are obtained from the indices of polarimetric purity (IPP), which can be extracted from the eigenvalues of a covariance matrix $\mathbf{H}(\mathbf{M})$. The PI is defined as a quadratic average of the IPP (with equal weights), which gives a meaningful interpretation of the scattering subregions of the plane. All the geometric properties of both the $\mathrm{PI} - P_\Delta$ and $S(\mathbf{M}) - P_\Delta$ planes are directly determined in terms of the values of the IPP. Furthermore, Monte Carlo simulations show that the so-called empty region (the subregion II) is filled in by the spherical Mie scatterer in backscattering, which is characterized by employing the characteristic decomposition. The $\mathrm{PI} - P_\Delta$ plane has a simpler geometric representation and is more convenient for the classification of the polarized light scattering media, and the analysis based on the IPP and the CD provide a deeper insight of the depolarization properties.

The work is supported by National Natural Science Foundation of China (NSFC) Grants No. 11374179 and No. 61527826. A. T. would like to acknowledge the Mirpur University of Science and Technology (MUST), Mirpur, AJ&K, Pakistan for granting him study leave.

*mahui@tsinghua.edu.cn

[1] M. Sun, H. He, N. Zeng, E. Du, Y. Guo, S. Liu, J. Wu, Y. He, and H. Ma, Characterizing the microstructures of biological tissues using Mueller matrix and transformed polarization parameters, Biomed. Opt. Express **5**, 4223 (2014).

[2] J. J. Gil and R. Ossikovski, *Polarized Light and the Mueller Matrix Approach* (CRC Press, Boca Raton, 2016).

[3] J. J. Gil, Review on Mueller matrix algebra for the analysis of polarimetric measurements, J. Appl. Remote Sens. **8**, 081599 (2014).

[4] J. J. Gil and E. Bernabéu, A depolarization criterion in Mueller matrices, Opt. Acta **32**, 259 (1985).

[5] R. Barakat, Polarization entropy transfer and relative polarization entropy, Opt. Commun. **123**, 443 (1996).

[6] C. Brosseau, *Fundamentals of Polarized Light: A Statistical Approach* (John Wiley, New York, 1998).

[7] A. Aiello and J. P. Woerdman, Physical Bounds to the Entropy-Depolarization Relation in Random Light Scattering, Phys. Rev. Lett. **94**, 090406 (2005).

[8] G. Puentes, D. Voigt, A. Aiello, and J. P. Woerdman, Experimental observation of universality in depolarized light scattering, Opt. Lett. **30**, 3216 (2005).

[9] H. D. L. Pires and C. H. Monken, On the statistics of the entropy-depolarization relation in random light scattering, Opt. Express **16**, 21059 (2008).

[10] I. S. José and J. J. Gil, Invariant indices of polarimetric purity: Generalized indices of purity for $n \times n$ covariance matrices, Opt. Commun. **284**, 38 (2011).

[11] J. J. Gil, Polarimetric characterization of light and media Physical quantities involved in polarimetric phenomena, Eur. Phys. J. Appl. Phys. **40**, 1 (2007).

[12] J. J. Gil, Components of purity of a Mueller matrix, J. Opt. Soc. Am. A **28**, 1578 (2011).

[13] T. Yun, N. Zeng, W. Li, D. Li, X. Jiang, and H. Ma, Monte Carlo simulation of polarized photon scattering in anisotropic media, Opt. Express **17**, 16590 (2009).

[14] H. He, N. Zeng, W. Li, T. Yun, R. Liao, Y. He, and H. Ma, Two-dimensional backscattering Mueller matrix of sphere-cylinder scattering medium, Opt. Lett. **35**, 2323 (2010).

[15] E. Du, H. He, N. Zeng, Y. Guo, R. Liao, Y. He, and H. Ma, Two-dimensional backscattering Mueller matrix of sphere-cylinder birefringence media, J. Biomed. Opt. **17**, 126016 (2012).

[16] P. Li, C. Liu, X. Li, H. He, and H. Ma, GPU acceleration of Monte Carlo simulations for polarized photon scattering in anisotropic turbid media, Appl. Opt. **55**, 7468 (2016).

[17] R. Barakat, Theory of the coherency matrix for light of arbitrary spectral bandwidth, J. Opt. Soc. Am. **53**, 317 (1963).

[18] C. Brosseau and A. Dogariu, Chapter 4 - Symmetry properties and polarization descriptors for an arbitrary electromagnetic wavefield, Prog. Opt. **49**, 315 (2006).

[19] S. R. Cloude, *Polarisation: Applications in Remote Sensing* (Oxford University Press, Oxford, United Kingdom 2009).

[20] D. Anderson and R. Barakat, Necessary and sufficient conditions for a Mueller matrix to be derivable from a Jones matrix, J. Opt. Soc. Am. A **11**, 2305 (1994).

[21] S. R. Cloude, Group theory and polarisation algebra, Optik (Stuttgart) **75**, 26 (1986).

[22] S. R. Cloude, Conditions for the Physical realisability of matrix operators in polarimetry, in *Polarization Considerations for Optical Systems II, SPIE Proceedings Vol. 1166* edited by R. A. Chipman (SPIE-International Society for Optical Engineering, Bellingham, WA, 1989).

[23] J. J. Gil, Characteristic properties of Mueller matrices, J. Opt. Soc. Am. A **17**, 328 (2000).

[24] J. J. Gil, On optimal filtering of measured Mueller matrices, Appl. Opt. **55**, 5449 (2016).

[25] J. Yang, Y. Chen, Y. Peng, and H. Yamada, New formula of the polarization entropy, IEITC Trans. Commun. **89**, 1033 (2006).

[26] Y. Wang, J. Chang, C. He, S. Liu, M. Li, N. Zeng, J. Wu, and H. Ma, Mueller matrix microscope: a quantitative tool to facilitate detections and fibrosis scorings of liver cirrhosis and cancer tissues, J. Biomed. Opt. **21**, 071112 (2016).

[27] C. Brosseau, Mueller matrix analysis of light depolarization by a linear optical medium, Opt. Commun. **131**, 229 (1996).

[28] D. Bicout and C. Brosseau, Multiply scattered waves through a spatially random medium: entropy production and depolarization, J. Phys. I (France) **2**, 2047 (1992).

[29] C. Brosseau and D. Bicout, , Entropy production in multiple scattering of light by a spatially random medium, Phys. Rev. E **50**, 4997 (1994).